OPEN ACCESS Freely available online

PLOS ONE

Growth Decline Linked to Warming-Induced Water Limitation in Hemi-Boreal Forests

Xiuchen Wu[1]*¤, Hongyan Liu[1]*, Dali Guo[1], Oleg A. Anenkhonov[2], Natalya K. Badmaeva[2], Denis V. Sandanov[2]

1 Department of Ecology, College of Urban and Environmental Sciences, Peking University, Beijing, China, **2** Institute of General and Experimental Biology, Siberian Branch of the Russian Academy of Sciences, Ulan Ude, Russia

Abstract

Hemi-boreal forests, which make up the transition from temperate deciduous forests to boreal forests in southern Siberia, have experienced significant warming without any accompanying increase in precipitation during the last 80 years. This climatic change could have a profound impact on tree growth and on the stability of forest ecosystems in this region, but at present evidence for these impacts is lacking. In this study, we report a recent dramatic decline in the growth of hemi-boreal forests, based on ring width measurements from three dominant tree-species (*Pinus sylvestris, Larix sibirica* and *Larix gmelinii*), sampled from eight sites in the region. We found that regional tree growth has become increasingly limited by low soil water content in the pre- and early-growing season (from October of the previous year to July of the current year) over the past 80 years. A warming-induced reduction in soil water content has also increased the climate sensitivity of these three tree species. Beginning in the mid-1980s, a clear decline in growth is evident for both the pine forests and the larch forests, although there are increasing trends in the proxy of soil water use efficiencies. Our findings are consistent with those from other parts of the world and provide valuable insights into the regional carbon cycle and vegetation dynamics, and should be useful for devising adaptive forest management strategies.

Citation: Wu X, Liu H, Guo D, Anenkhonov OA, Badmaeva NK, et al. (2012) Growth Decline Linked to Warming-Induced Water Limitation in Hemi-Boreal Forests. PLoS ONE 7(8): e42619. doi:10.1371/journal.pone.0042619

Editor: Gil Bohrer, Ohio State University, United States of America

Received December 21, 2011; **Accepted** July 10, 2012; **Published** August 15, 2012

Copyright: © 2012 Wu et al. This is an open-access article distributed under the terms of the Creative Commons Attribution License, which permits unrestricted use, distribution, and reproduction in any medium, provided the original author and source are credited.

Funding: This research was funded by the National Natural Science Foundation (40711120173) and Russian Foundation for Basic Research (06-04-39012). The funders had no role in study design, data collection and analysis, decision to publish, or preparation of the manuscript.

Competing Interests: The authors have declared that no competing interests exist.

* E-mail: xcwu@bgc-jena.mpg.de (XCW); lhy@urban.pku.edu.cn (HYL)

¤ Current address: Max Planck Institute for Biogeochemistry, Jena, Germany.

Introduction

Boreal forests in the northern hemisphere are predicted to be a major sink for atmospheric CO_2 as the global climate warms [1,2]. Satellite observations, atmospheric CO_2 measurements and the results of dynamic vegetation models have shown that climate warming leads to increased tree growth and a marked greening trend in boreal forests [3,4,5]. However, there are also reports of extensive tree growth decline or mortality at northern mid- and high- latitudes [6,7,8,9], which highlights the large tempo-spatial variability in tree growth responses to climate change in boreal forests [10].

Given that tree growth is apparently declining rapidly in many parts of the world, even under relatively modest increases in global mean temperature and a drying climate [8], broad-scale climate-induced stress on tree growth could be expected to accompany projected future climate patterns [11]. In particular, warming-induced drought may trigger an extensive decline in the growth of hemi-boreal forests. A recent study showed that the decline in growth of *Larix siberica* in hemi-boreal forests is closely related to increased drought stress [9]. However, it is far from clear about the responses of tree growth to potential warming-induced drought.

Climate change models predict warmer temperatures in the hemi-boreal forests of southern Siberia [11], where there are three dominant species (*P. sylvestris, L. sibirica* and *L. gmelinii*). This warming may trigger a reduction in soil water content, thus further constraining tree growth and potentially leading to profoundly altered forest dynamics, such as large-scale tree die-off [8]. Previous studies have also found that the warming-induced decline in growth persists despite the fact that the water use efficiency of trees shows an increasing trend in many regions [12,13,14]. This background leads to two critical questions: (1) Has growth decline occurred in this region, and if so, what are the driving forces for this decline? (2) Do the responses of tree growth to climate differ between different species linked to the stand conditions? To answer these questions, we examined the relationship between tree growth and climate over the past 80 years in this region, based on a tree ring network (Fig. 1A). Answers to these questions will provide us with insights into the regional carbon cycle, vegetation dynamics and forest management in this and other hemi-boreal forests world-wide.

Results

Temporal Trends in Tree Growth and Common Variance

The BAI series consistently tracked the standardized TRI series for all three species between 1928 and 2006 (Figs. 2A, C, E). Trends in the BAI and TRI series show that *P. sylvestris* has undergone a remarkable decline in growth since 1928, despite the high variability highlighted by the smoothing fitted cubic spline

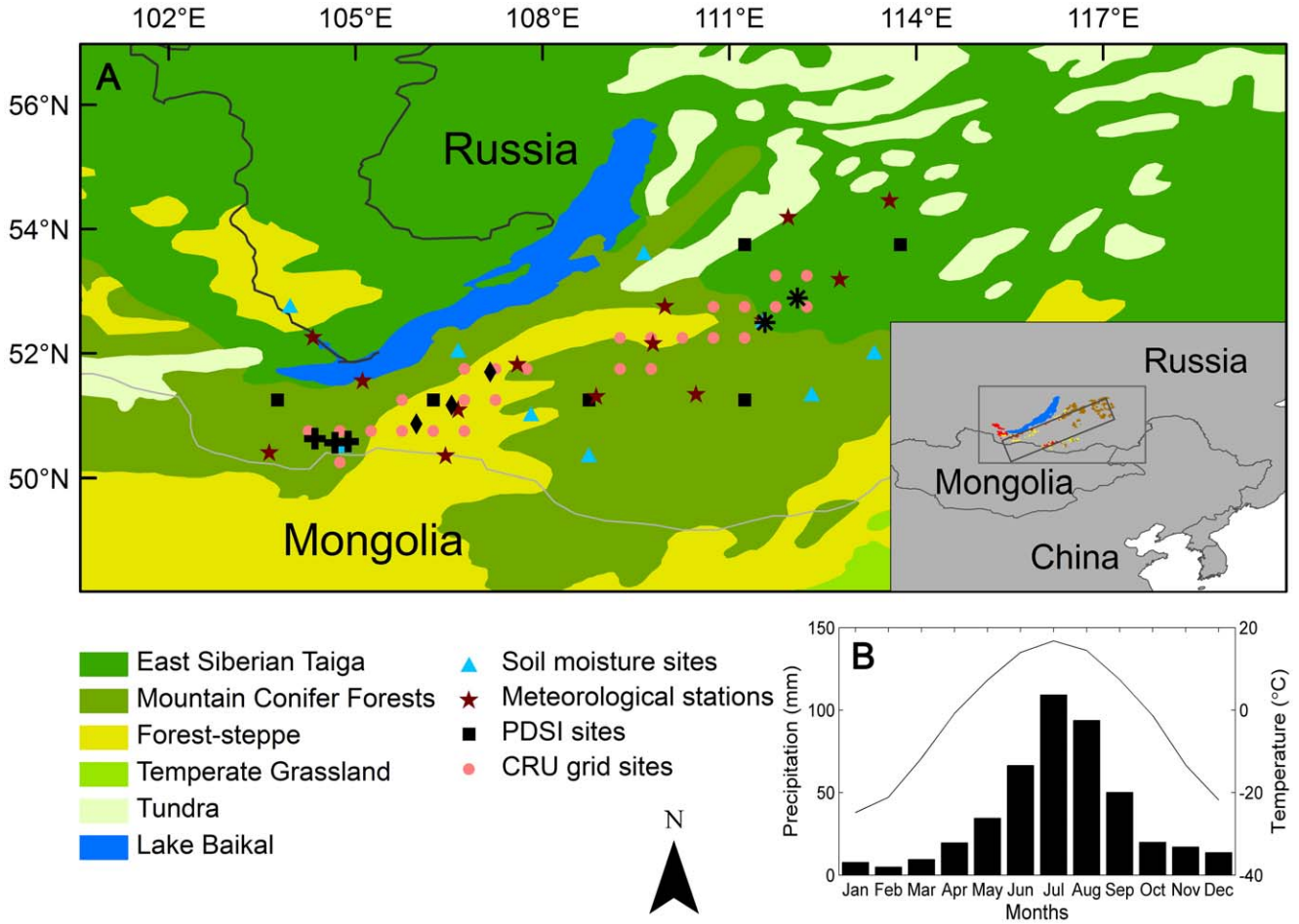

Figure 1. Geographical position (A) and climate diagram (B) of the study region. The sample sites of *Larix sibirica*, *Pinus sylvestris* and *Larix gmelinii* are indicated by black crosses, black diamonds and black asterisks, respectively. The approximate location of the selected transect (as indicated by the italic rectangle) and schematic distribution (according to the Forests of the USSR Map, 1990) of the three species (*L. sibirica*, *L. gmelinii* and *P. sylvestris*, as indicated by red, brown and yellow small patches, respectively) in and around the transect are shown in the inlet figure in (A). The mean monthly temperature (line) and total monthly precipitation (bars) during 1928–2006 are shown in (B) with data derived from dataset CRU TS 3.0 (http://www.cru.uea.ac.uk/).
doi:10.1371/journal.pone.0042619.g001

(Figs. 2A). In contrast, the tree growth for larch species appears to have remained relatively stable (*L. gmelinii*), or even to have increased (*L. sibirica*), during these early periods (e.g. before the mid-1980s), and to have suffered a dramatic decline over the last 20 years of the record (Figs. 2C, E). The fitted linear regression shows the decline rates of BAI to be 0.70 ($p<0.05$) and 0.78 cm^2 per decade ($p<0.05$) for *L. sibirica* and *L. gmelinii* for the last two decades (1986–2006) respectively. Overall, although temporal changes in growth patterns differ between these three species, all have experienced a decline in growth since approximately the middle of 1980s. Negative anomalies in the TRI series also appear to have been becoming increasingly prominent over the last two decades (Fig. 2B, D, F). The stand-level basal area increment measures of tree growth show close positive relationships to the growing season average NDVI for the period 1982–2006 for all the three species, as can be seen from the linear regression fits (Fig. 3). This result demonstrates that our sample data is representative of larger scale tree growth patterns in the region, and suggests that the hemi-boreal forests may be suffering a recent dramatic decline in growth, which has been especially severe since the late 1980s.

The first and second PCs (PC1 and PC2) of the chronology network PCA are significant, representing 42.1% and 18.7% of the total variance respectively. The scatter plot of the PCA loading coefficients reveals groups of chronologies with similar growth patterns (Fig. *S3*). Although the 8 chronologies are associated with different loadings for PC1, all 8 are positively correlated with it, showing that they share a common variance. *P. sylvestris* chronologies were mainly negatively correlated with PC2, while the two larch species chronologies generally had a positive correlation with PC2 (Fig. *S3*). The shared growth variability (PC1) for all the chronologies shows a marked increase ($r^2 = 0.38$, $p<0.05$) for recent decades (Fig. 4A).

Regional and Species Growth-climate Relationships

Correlation analyses between the first principle component (PC1) and mean monthly temperature show that the monthly temperature significantly affects tree growth only in December of the previous year and January of current year for the study period (Fig. 4B). In contrast, all monthly PDSI values between October of the previous year and July of the current year are significantly related to regional tree-growth (Fig. 4C). The results of the step-wise linear regression between PC1 and

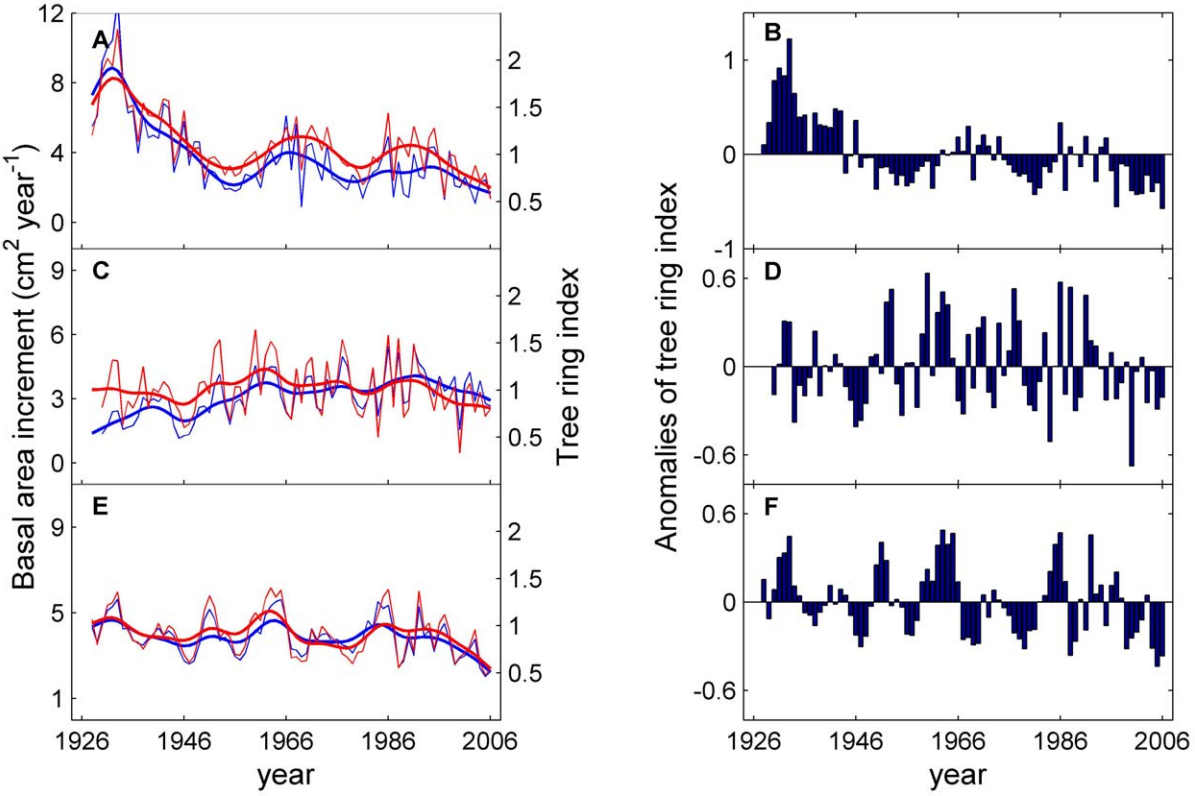

Figure 2. Basal area increments (blue lines), tree ring indices (red lines) and the anomalies of tree ring indices (bars) for *P. sylvestris* (A and B), *L. sibirica* (C and D) and *L. gmelinii* (E and F). Bold lines in the figure are the fitted cubic smoothing splines for basal area increments and tree ring indices.
doi:10.1371/journal.pone.0042619.g002

monthly-, growing season-, pre-growing season (October of the previous year to April of the current year)- average temperature and PDSI, as well as PDSI for October to July ($PDSI_{OCT\text{-}Jul}$), show that $PDSI_{OCT\text{-}Jul}$ contributed most to the variability in regional tree growth between 1937 and2005 ($p<0.05$). The close relationship found between the regional BAI and $PDSI_{OCT\text{-}Jul}$ confirms our results (Fig. 4D).

We further assessed the growth-climate relationships for the three species and identified some clear differences between the tree growth-climate responses of *P. sylvestris* and that of the two larch species. The tree growth of *P. sylvestris* is significantly limited (negative correlation) by the mean monthly temperature in the months during, and immediately prior to, the growing season, e.g. March, May, June and September (Fig. 5A). Conversely, larch tree-growth does not appear to be significantly affected by changes in temperature (*L. sibirica*), and seems to be limited by mean monthly temperature only during the pre- and early growing season, e.g. April and June (*L. gmelinii*) (Figs. 5B, C). Precipitation during both the growing season (e.g. June and July) and the pre-growing season (e.g. previous November) had a great effect on tree growth for *P. sylvestris* (Fig. 5A). In contrast, the larch growth is only correlated significantly to the precipitation for the growing season (Figs. 5B, C). *P. sylvestris* shows a significant and positive correlation to PDSI for all months, which differs from the results for larch, which show a significant and positive correlation to PDSI for the pre- and early growing season (Figs. 5A–C).

Climate Sensitivity of Tree Growth

Despite high interannual variation, the mean sensitivity of *L. sibirica* and *L. gmelinii* increased markedly over the period 1928–2006, as illustrated by the results of both Mann-Kendall test (Z values are 2.44 and 2.24, respectively) and the linear regression fits (Figs. 6C, E). The P_{SWUE} of all three species increased dramatically from 1937 to 2005, as illustrated by the Mann-Kendall trend test (Z values are 5.86, 4.09 and 2.07 respectively, $p<0.05$) and by the linear regression fits (Figs. 6B, D, F).

Climate Trends and Warming-induced Soil Water Limitation

Significant increases were seen in nearly all monthly temperatures during this period, as shown by the Mann-Kendall test. The estimated linear rate of temperature increase ranges from 0.13°C per decade in August to 0.51°C per decade in February, when considering data spanning the last 80 years (data are not shown here). The most dramatic increase in temperature was seen in the pre- and early growing season. No obvious trends were evident in the total monthly precipitation for the same period (except marked decreases in February and March, with linear slopes of −0.03 and −0.05 mm year^{-1} respectively), despite the high variability evident in the record. Notably, all monthly PDSI series have decreased markedly since 1937.

The $PDSI_{OCT\text{-}Jul}$ has been undergoing a dramatic decline since 1937, as detected by the Mann-Kendall test and highlighted by a smoothing cubic spline and a linear regression fit (Fig. 7A, $y=-0.066x+129.1$, $r^2=0.42$, $p<0.05$). The modeled regional soil water limitation through October of the previous year to July of

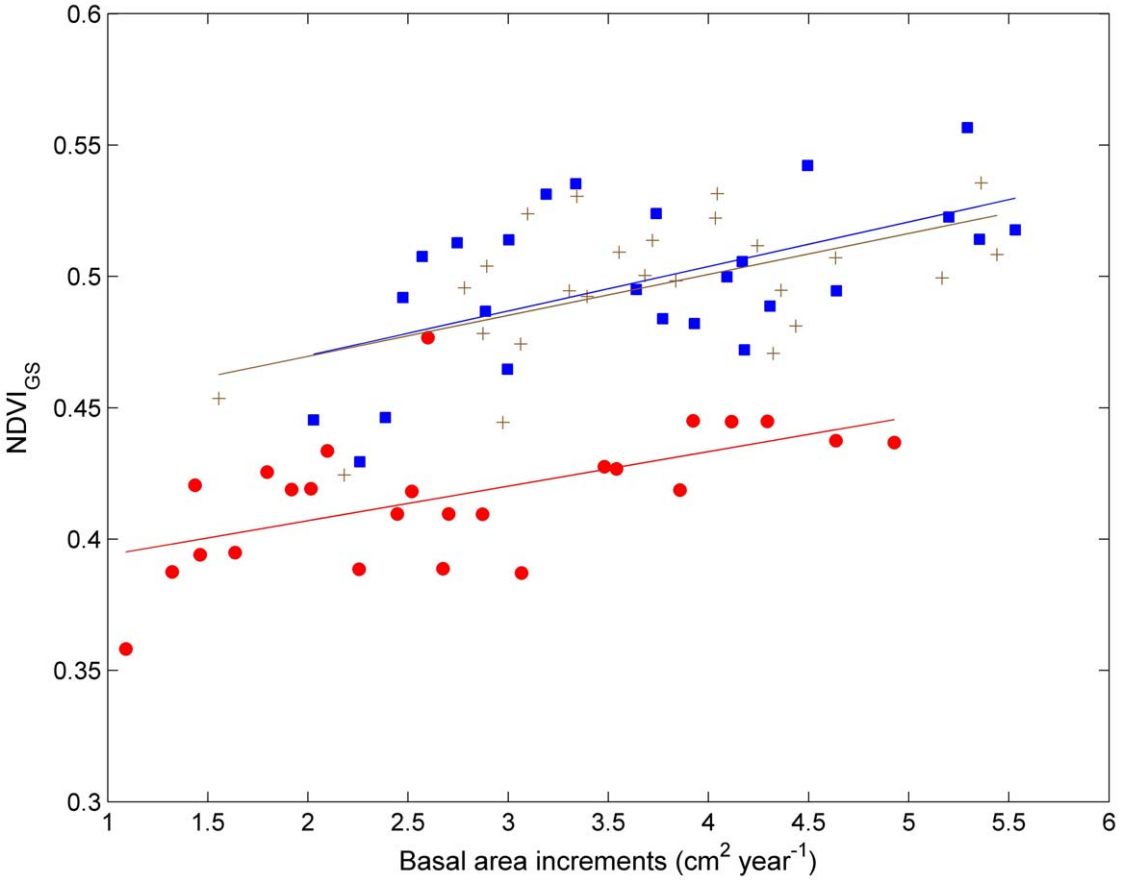

Figure 3. Basal area increments versus growing season average normalized difference vegetation index (NDVI) during 1982–2006 for *P. sylvestris* (red circle), *L. sibirica* (brown cross) and *L. gmelinii* (blue square). The lines are linear fits of the relationship between basal area increments and NDVI for *P. sylvestris* ($y = 0.38+0.013x$, $r^2 = 0.33$, $p<0.001$), *L. sibirica* ($y = 0.44+0.016x$, $r^2 = 0.30$, $p<0.001$) and *L. gmelinii* ($y = 0.44+0.017x$, $r^2 = 0.32$, $p<0.01$).
doi:10.1371/journal.pone.0042619.g003

the current year ($SWL_{OCT\text{-}Jul}$) shows a marked increase since 1928, despite the high variability evident in the record (Fig. 7B). In general, the $SWL_{OCT\text{-}Jul}$ for this region has increased at a rate of 9.4 mm per decade since 1928, as shown in the linear fit for $SWL_{OCT\text{-}Jul}$ (Fig. 7B, $y = -0.94x+1823.7$, $r^2 = 0.11$, $p<0.05$).

Discussion

Drought Stress and Regional Tree Growth Decline

The increasing soil water limitation through October of the previous year to July of the current year, as indicated by the significant decreasing $PDSI_{OCT\text{-}Jul}$ and increasing $SWL_{OCT\text{-}Jul}$ (Figs. 7A, B), is tightly linked to the substantial decline in growth of hemi-boreal forests in southern Siberia, as demonstrated by the close relationships between regional tree growth and monthly PDSI and $PDSI_{OCT\text{-}Jul}$ (Figs. 4C, D). The increasing soil water limitation has become more limiting to regional tree growth, which is indicated by the marked increase in the shared growth variance held by the chronologies of these three species (Fig. 4A), and by the matching trends in regional BAI and $PDSI_{OCT\text{-}Jul}$ (Fig. 4D). These results suggest that drought stress limits the tree growth of hemi-boreal forests in our study region. Some previous studies in nearby regions have obtained similar results and corroborate this conclusion [9,15,16,17,18]. For instance, tree growth of *L. sibirica* in northern Mongolia [9] as well as that of *L. gmelinii* in central Siberia [18], was shown to decrease with increasing drought stress during the growing season. Notably, tree growth decline due to warming-induced drought stress is evident at mid- and even high- latitude areas of the Northern Hemisphere [6,7,8,12,19]. Taken together, these results support the hypothesis that drought-stress may accompany increased warming in the boreal forest [6,19].

Why does temperature warming result in drought stress in hemi-boreal forests in southern Siberia and thus limit tree growth? Temperature increases are stronger in the pre- and early growing seasons in southern Siberia, without concurrent increases in precipitation. This leads to a marked increase in evaporation and, therefore, a dramatic decrease in soil water content (Fig. 7A) and an increase in soil water limitation (Fig. 7B). The dramatic increase in temperature during the pre- and early growing season may exacerbate the soil water limitation by degrading the permafrost [20,21,22] and reducing snow cover in our study region [23], whereas permafrost and snow melt could have a considerable effect on tree growth in this region [24,25,26]. Therefore, the pronounced warming, particular during the pre- and early growing seasons, appears to trigger a marked increase in soil water limitation in southern Siberia, which, in turn, has led to a recently marked decline in tree growth for these forests (Figs. 2A–F), notwithstanding that there are increasing trends in a proxy of soil water use efficiency (Fig. 6B, D, F). These results also highlight the important effect of environmental conditions before, and at the

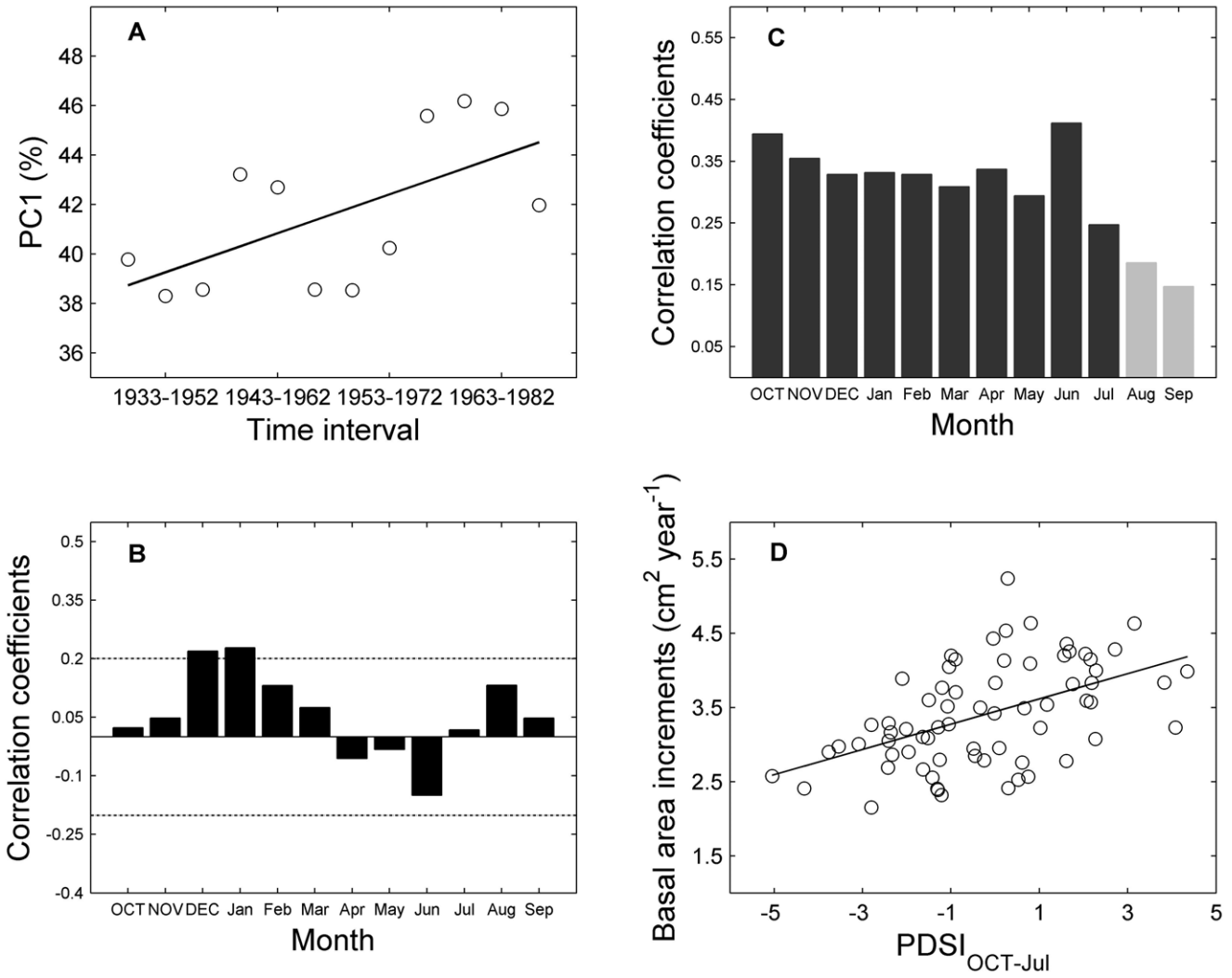

Figure 4. Evolution of shared growth variability explained by the first principal component (PC1) and relationships between PC1 and climate. Evolution of shared growth variability (estimated by the PC1) since 1928 using subintervals of 20 years with a 5-year lag was shown in (A) with a linear fit (black line, $y = 0.53x+38.21$, $r^2 = 0.38$, $p = 0.032$). Simple correlations performed between the first principal component (PC1) and monthly temperature during 1928–2006 (B) and PDSI during 1937–2005 (C). The dotted lines in (B) indicate the 95% confidence intervals. Dark grey bars in (C) are statistically significant ($p<0.05$). The relationship between the regional BAI series and the average PDSI values through October of prior year to July of current year during 1937–2005 was shown in (D) with a linear fit (black line, $y = 0.17x+3.45$, $r^2 = 0.25$, $p<0.001$).
doi:10.1371/journal.pone.0042619.g004

very beginning of, the growing season on tree growth and vegetation activity in hemi-boreal forests. Previous studies corroborate this conclusion and have shown that tree growth for *L. sibirica* in this region is mainly controlled by the precipitation received early in the growing season [27].

Clearly, we found no evidence for the widely-observed vegetation greening trends reported for the past two decades for southern Siberia [4,5]. Instead we found evidence for a "browning" phenomenon, as indicated by the common decline in tree growth for these three dominant species over the last two decades (Figs. 2A–F). Remote sensing observations have revealed that the forested areas across northern circumpolar high latitude regions (above 50°N) have also suffered a gross "browning" trend in recent decades (i.e. during early 1980 s to early 2000 s) [28,29,30], particularly in the late summer, due to warming-induced drought [30].

The marked recent decline in tree growth for the three dominant species in hemi-boreal forests (Figs. 2A–F) due to warming-induced drought stress suggests that, under climate warming, the carbon uptake in this region may be stalled or even reversed, which would act as a positive feedback effect for climate warming [31]. If this limitation in growth due to drought stress is sustained, the future capacity of hemi-boreal forests to sequester carbon may be less than currently expected, although many other components of the carbon balance need further investigation. More importantly, increasing soil water limitation appears to have constrained forest regeneration [9,17,32] and increased the climate sensitivity of tree growth in this region (Figs. 6B–F). These results suggest that tree growth in this region is becoming more vulnerable to climate warming [9,17,32]. The present study, combined with previous results [9,32], also suggests that the hemi-boreal forests will retreat if faced with more severe drought stress in the future.

Climate change will also indirectly alter forest dynamics through the effect on disturbance regimes [33,34]. In boreal forests, the currently dominant disturbances are fire [35] and insects [36].

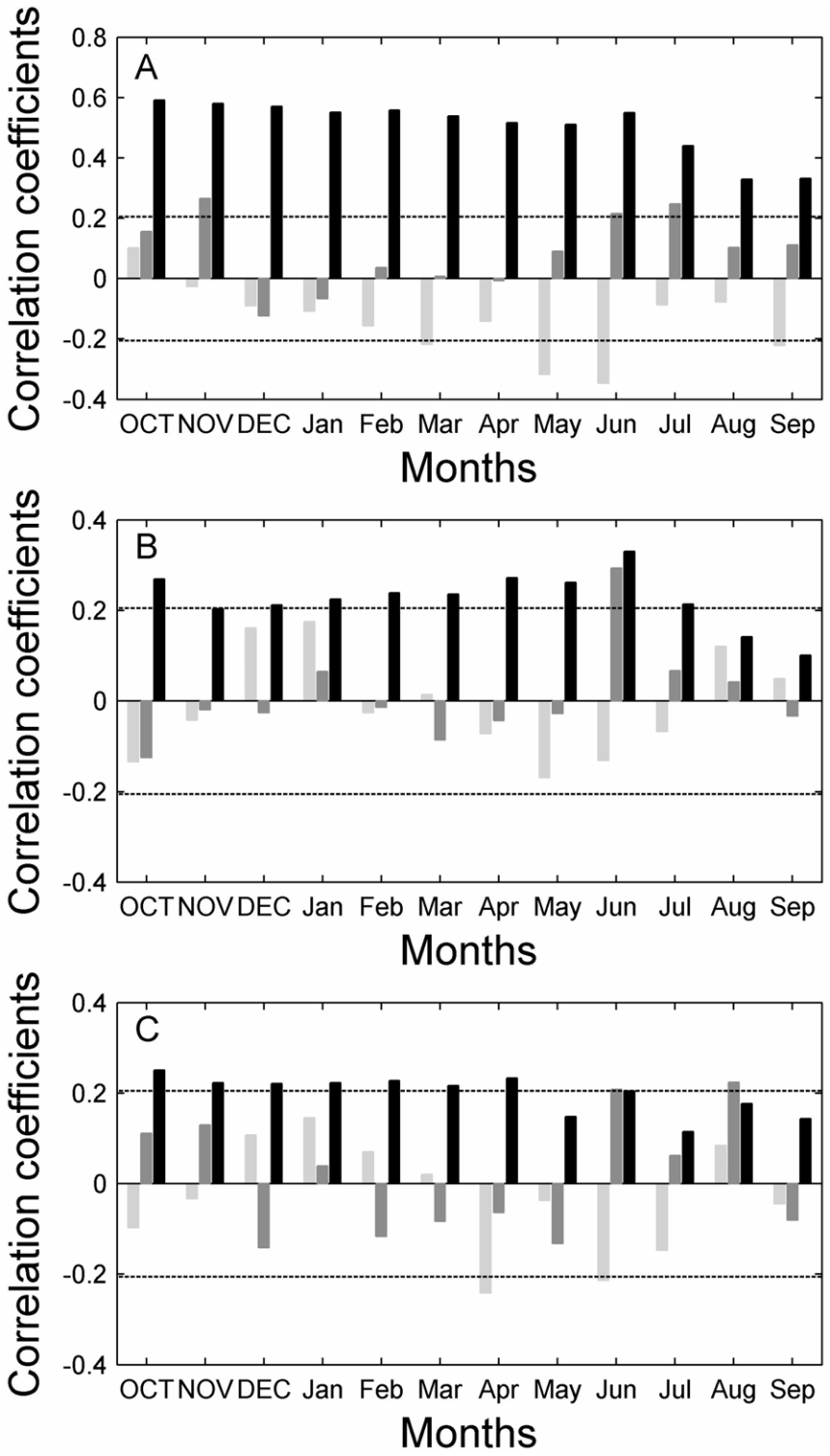

Figure 5. Correlations between the standard chronology and temperature (light grey bars), precipitation (dark grey bars), and PDSI (black bars) during 1937–2005 regarding *P. sylvestris* (A), *L. sibirica* (B) and *L. gmelinii* (C). The dotted lines indicate the 95% confidence intervals.
doi:10.1371/journal.pone.0042619.g005

Although the recent common decline in tree growth for these three tree species cannot be linked to fire or insect disturbance (due to the lack of any evidence of fire, e.g. fire scars on trees or charcoals in the soil sediments), or to insect prevalence in our sampling sites, the incidence and severity of fires and insects is likely to increase with increased aridity [37,38]. These disturbances, combined with warming-induced drought stress, may have a multiplicative effect on forest dynamics in hemi-boreal forests.

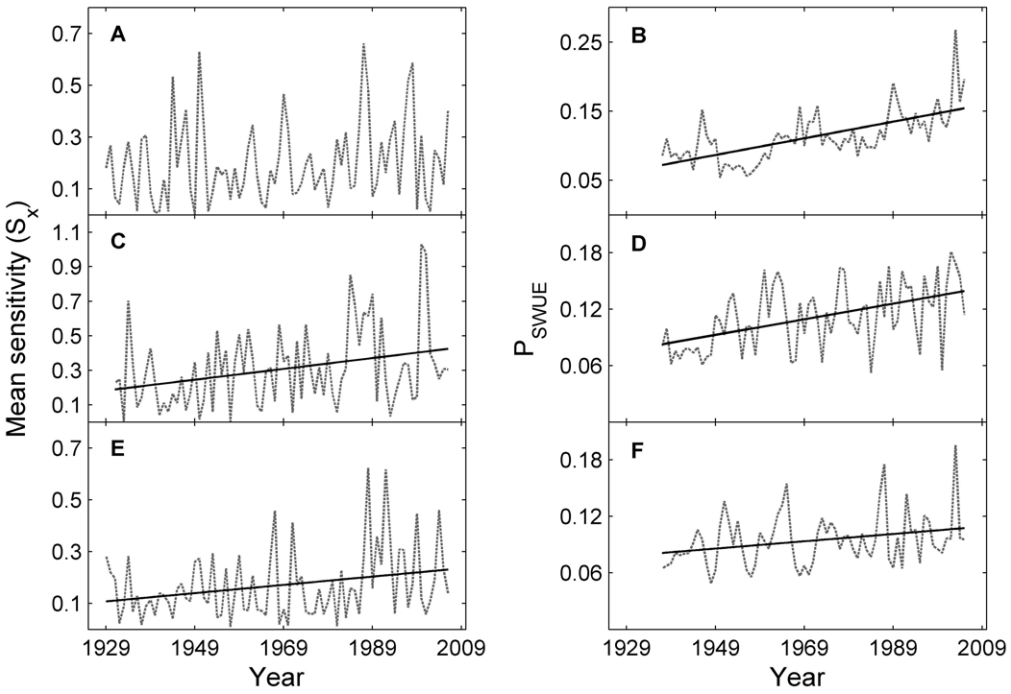

Figure 6. Temporal changes of mean sensitivity (S_x, 1928–2006) and a proxy of soil water use efficiency (P_{SWUE}, 1937–2005) relating to *P. sylvestris* (A, B), *L. sibirica* (C, D) and *L. gmelinii* (E, F). Lines in this figure are linear fits of S_x and P_{SWUE} for *P. sylvestris* ($y = 0.0012x–2.26$, $p<0.001$), *L. sibirica* ($y = 0.0027x–4.93$, $p<0.05$, $y = 0.00083x–1.53$, $p<0.001$) and *L. gmelinii* ($y = 0.0016x–2.97$, $p<0.05$; $y = 0.00033x–0.55$, $p<0.05$) if there are significant trends as detected using Mann-Kendall test.
doi:10.1371/journal.pone.0042619.g006

Different Growth-climate Responses Among Species Linked to Stand Conditions

The growth response of different species to climate changes in the region differed, with the most obvious difference being between *P. sylvestris* and the two larch species. Comparisons of the growth-climate relationships found for individual species show that *P. sylvestris* growth tends to be more limited by soil water limitation than growth for the larch species (Figs. 5A–C). Several factors, such as differences in the fire and insect regime, tree density, stand-level water conditions and drought resistance capacity, can contribute to differences in tree growth patterns and to growth-climate relationships. As mentioned above, we did not find any evidence of fire or insect disturbance at any of our sampling sites, therefore the different tree growth pattern and growth-climate relationship cannot be linked to the difference between the fire and insect regimes for the pine and larch forests. In addition, the tree density of the pine forests (canopy cover of 25%∼35%) is much lower than that of the larch forests (canopy cover of 50%∼70%), indicating that the more severe drought stress (Fig. 5A) in pine forests can not be attributed to higher tree competition. Instead, these differences may be largely due to differences in stand-level water conditions and the drought resistance capacity inherent in each species.

P. sylvestris growing in the forest–steppe ecotones exhibits conservative water consumption with a sensitive stomatal regulation and relatively constant shoot water potentials under dry conditions [39]. It has a much lower transpiration rate (0.06–0.18 $g.g^{-1}\ h^{-1}$) than the two larch species (*Larix sibirica* 0.06–0.54 $g.g^{-1}\ h^{-1}$ and *Larix gmelinii* 0.10–1.08 $g.g^{-1}\ h^{-1}$) [40]. These results suggest that *P. sylvestris* has greater drought resistance [39,40].

The *P. sylvestris* forests are generally located on the north-facing slopes of mountains in the forest-steppe ecotones, where permafrost islands seldom melt within the valley bottoms, which are covered by peaty soils. Therefore, *P. sylvestris* trees at the sampling sites are not influenced by permafrost but are only influenced by the seasonal frozen soil [41]. In winter a seasonal soil freezing up to a depth of 2–2.5 m occurs [41]. In comparison, the larch forests are generally located in a zone with sporadic permafrost (*L. sibirica*) or discontinuous permafrost (*L. gmelinii*), with a permafrost depth of 50–80 m and 120–130 m, and mean annual temperature of −0.2 to −1°C and −1.2 to −1.7°C respectively [41]. During summer, the depth of the active layer of permafrost is 1.5–2.5 m [41,42]. A previous study has proven that permafrost can be a direct source of water for plants under severe drought stress, and can retain surplus water in the soil until the next summer [24]. Therefore, the larch forests could benefit from the permafrost, especially during the mid to late growing season [24]. Although the pine forests could also benefit from seasonal frozen soil, there are two reasons that they may face a more severe drought. Firstly, the pine forests are located in a drier region, which suffers from a more rapid early spring warming (unpublished data from our group), leading to a much earlier melting of the seasonal frozen soil, and thus to drier soil conditions due to evaporation and possible runoff in the well-drained soil. Secondly, the organic layer depth is much shallower (0∼2 cm) in the pine forest areas than in the larch forests areas (5∼10 cm). This difference makes the melting of the seasonal frozen soil in pine forests easier and causes it to occur earlier than the analogous melting of permafrost in larch forests, because the net effect of the organic layer is to lower the soil temperature and decrease the seasonal thaw depth [22]. Taken together, differences in soil water conditions are probably the main explanation for the

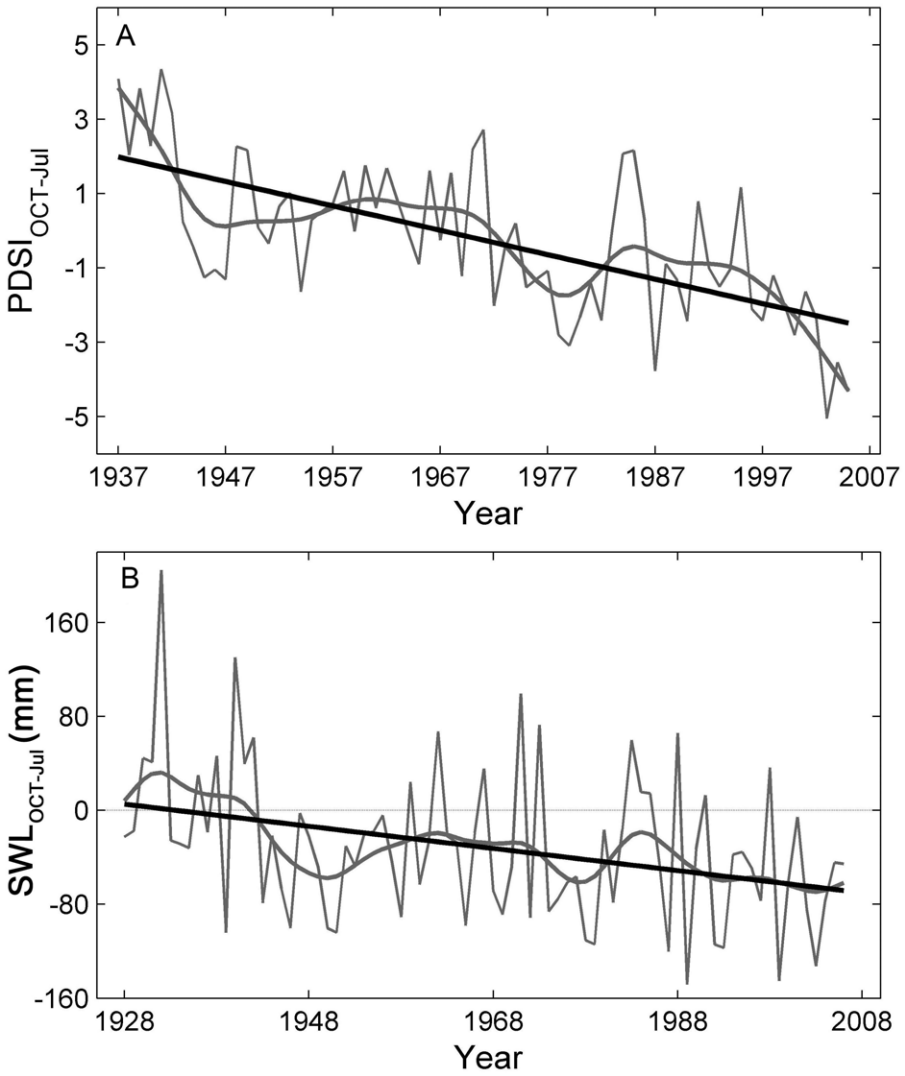

Figure 7. Changes of PDSI and soil water limitation in this region. Average PDSI values through October of prior year to July of current year during 1937–2005 (thin grey line) with a cubic smoothing spline (bold grey line) and a linear fit (black line, $y = -0.066x+129.1$, $p<0.001$) are shown in (A). Modeled regional soil water limitation through October of prior year to July of current year ($SWL_{OCT-Jul}$) during 1928–2006 (light grey line) with the cubic smoothing spline (bold grey line) and a linear fit (black line, $y = -0.94x+1823.7$, $p<0.01$) are shown in (B).
doi:10.1371/journal.pone.0042619.g007

different tree growth responses to the changing climate between the Scots pine and larch.

These results can give us some insight into vegetation dynamics [43] and can be useful for the devising of adaptive forest management strategies for this region. With increasing drought stress (Figs. 7A, B) and climate sensitivity (Figs. 6A, B), *P. sylvestris*, which dominated the forest-steppe ecotone, is currently unable to encroach on the steppe in this region. Predicted stronger climate warming trends [11] could result in a retreat of the pine forest in the forest-steppe ecotones due to more severe warming-induced drought stress. The larch forests in this region will become more vulnerable when facing increased climate warming and will suffer a long-lasting decline in growth. In addition, if a retreat of the permafrost were to accompany the warming climate, a reduction in these forests could follow [44]. However, redistribution of forest zones and their dominant climates will require long periods of adjustment for the amount of change being predicted [44]. Given the potential risks of climate-induced forest decline, increased attention should be paid to forest management for this region. For the much denser larch forests, a light thinning management, which moderates competition for water between trees, could be an alternative option for enhancing forest resistance and resilience to increasing climate stress [45]. For the pine forests (with canopy cover of 25~35%), we advise selecting more drought-resistant genotypes to adapt the drier soil conditions that *Pinus sylvestris* is facing [46].

Materials and Methods

Study Area and Sample Collection

The sample area was a northeast-southwest transect in the Trans-Baikal region, which is located at the southern limit of the boreal forest, also called hemi-boreal forest (Fig. 1A). Three widely distributed coniferous species, *Larix sibirica*, *L. gmelinii* and *Pinus sylvestris*, which dominate the Trans-Baikal coniferous forests, East Siberian taiga and Selenge-Orkhon forest steppe, respectively, are found in this region. Forests in this area are generally fragmented and distributed on the north-facing slopes of mountains. Pine

forests are generally located in much drier regions than larch forests. In addition, the canopy cover of pine forests (25%~35%) is much lower than that of larch forests (50%~70%). The soil is coarse-textured and poor in nutrients, with a total nitrogen content ranging from 0.5 to 2.7 g/kg and a total carbon content ranging from 10 to 38 g/kg.

The climate in this region is continental. Mean annual precipitation is about 446 mm. July (mean temperature of 16.7°C) and January (mean temperature of −24.8°C) are the warmest and coldest months respectively (Fig. 1B). The growing season is approximately May-September, during which about 79% of the mean annual precipitation is received. In addition, there are discontinuous areas of permafrost in our study region, with the mean annual ground temperature ranging from 0 to −2°C [22].

Tree-ring samples from three different tree species were collected from 8 representative stands of 25 × 25 m^2 (Fig. 1A). In these selected stands human and animal disturbance (e.g. grazing, logging) is minimal (few stumps and no feces evident). In addition, we found no evidence of disturbance by insects or fire (no fire scars evident on trees or charcoals in the soil profiles). However, we cannot be certain of the disturbance regime of these forests before tree establishment. The primary objective of this study is to evaluate patterns of tree growth in this region, and to assess their relationship to climate change. In each stand, we sampled all trees with a d.b.h (diameter at breast height) greater than 10 cm unselectively using an increment borer at a height of 1.3 m. In general, 30–80 individuals were sampled from each stand. Two cores were taken from each tree. The geographical features of the sampling sites are shown in Table 1. Notably, no specific permits were required for the presented field studies, and the field studies did not involve endangered or protected species.

Chronology Construction and Tree Growth Evaluation

All samples were cross-dated, measured (with precision to the nearest 0.01 mm, using the LINTAB system) and processed using standard dendrochronological techniques [47,48]. Using the program ARSTAN, we applied conservative detrending methods, based primarily on the negative exponential function or on a fitted linear regression with any slope for each raw measurement series, to remove non-climatic and tree-age-related growth trends [49]. Tree ring indices (TRI) were obtained by dividing the observed ring-width value by the predicted ring-width value. For each stand, the TRIs were averaged by year using a bi-weighted robust mean to construct a standard chronology. The Expressed Population Signal (EPS), with a threshold set at 0.85, was used to determine the most reliable time span for the chronologies [50,51]. We then constructed the standard ring-width chronologies for the three different tree species by averaging the standard chronologies for the relevant sites to determine the tree growth trend and annual variability. Descriptive statistics are presented to allow comparisons of the sites with other dendroclimatic data sets (Table 1).

Given the bias intrinsic to investigating tree growth trends on the basis of changing tree ring indices alone [52], we compared and combined the basal area increment (BAI) and tree ring indices to evaluate long-term changes in growth [52,53,54]. BAI is far less dependent on changes in tree age/size and is a good indicator of forest growth and productivity [53,54].

Stem BAI was computed using the cross-dated ring width series. Past annual BAI was estimated by subtracting twice the annual ring width from the annual outside bark diameter [12]. Raw BAI chronologies for the three species were built as the average by year of individual-tree BAI series to establish the long-term growth trends. Smoothing cubic spline functions were fitted to the BAI and ring-width chronologies for the three species using MATLAB, in order to highlight the long-term growth trends.

The high quality GIMMS (Global Inventory Modeling and Mapping Studies) dataset of the normalized difference vegetation index (NDVI) [55,56] was compared to the species BAI series. Since NDVI has been demonstrated to be a high quality indicator of large-scale trends in vegetation activity, this comparison allowed

Table 1. Geographic features and chronology statistics for our study sites.

Sites						Chronology†				
Site ID	Latitude (N)	Longitude (E)	Altitude (m)	Slope	Slope Degree	No. Trees	No. Radii	ms_x	*R*	Reliable*
										Time Span
L. sibirica						178	306	0.428	0.675	1928–2006
Plot A	50.63°	104.35°	858	NE 25°	26°	84	168	0.42	0.84	1923–2006
Plot B	50.57°	104.67°	1035	NE 0°	15°	45	87	0.43	0.573	1924–2006
Plot C	50.58°	104.88°	876	NE 0°	20°	49	69	0.452	0.775	1928–2006
P. sylvestris						87	165	0.432	0.515	1910–2006
Plot D	50.87°	105.98°	920	NE 50°	15°	35	55	0.473	0.871	1900–2006
Plot E	51.16°	106.54°	834	NE 20°	15°	58	103	0.36	0.553	1928–2006
Plot F	51.70°	107.16°	751	NE 30°	20°	27	45	0.45	0.575	1927–2006
L. gmelinii						120	200	0.423	0.523	1928–2006
Plot G	52.49°	111.58°	1038	NE260°	10°	54	92	0.372	0.504	1910–2006
Plot H	52.89°	112.10°	991	NE17°	3°	44	81	0.311	0.573	1892–2006

Note:
†Standard ring-width chronologies were developed for eight stands (A-H) using conservative detrending methods based primarily on the negative exponential function or linear regression with any slope. Species-specific standard chronologies were developed for *L. sibirica*, *L. gmelinii* and *P. sylvestris*, respectively.
*We determined the reliable time span for built chronologies according to the criteria of EPS (Expressed Population Signal) >0.85.
doi:10.1371/journal.pone.0042619.t001

us to assess whether the sample data obtained here are representative of larger scale tree growth patterns [57].

Climate Data

Observed climate data from the nearest stations (Fig. 1A) were obtained from the National Climatic Data Center (NCDC, http://www.ncdc.noaa.gov/). However, most available climate records in this region are only available after 1947, and are surprisingly discontinuous, and so cannot be straightforwardly matched for the period for our growth data (1928–2006). To gain a more thorough understanding of the relationship between climate and tree growth, we introduced a monthly gridded dataset from the Climate Research Unit (CRU TS 3.0, 1901–2006), with a regular latitude-longitude resolution of $0.5^\circ \times 0.5^\circ$ (CRU, http://www.cru.uea.ac.uk/) [58]. Regional monthly temperature and precipitation data derived from CRU TS 3.0 appear highly similar to the instrumental records from meteorological stations in this region for 1950–2006, with correlation coefficients for monthly temperature ranging from 0.89 ($p<0.000001$) in September to 0.98 ($p<0.000001$) in March, and for monthly precipitation ranging from 0.68 ($p<0.001$) in January to 0.92 ($p<0.000001$) in August. Based on a careful comparative analysis, monthly temperature and precipitation data from 1928 to 2006 were derived from the nearest grid cells of CRU TS 3.0 (Fig. 1A).

Monthly Palmer Drought Severity Indices (PDSI) for 6 grids (Fig. 1A) from 1937 to 2005 were derived from a global PDSI dataset with a spatial resolution of $2.5^\circ \times 2.5^\circ$ [59]. The PDSI is a good indicator of long-term regional soil water conditions because it incorporates the coupling effects of precipitation, temperature, and potential evapotranspiration [59,60,61], which are generally considered to be sensitive, low-noise indicators of large-scale interannual variations in soil water content in central Asia [59,60]. We also compared and validated the PDSI using the available gravimetric measurements of soil water contents in our study region.

We obtained monthly soil moisture observations for the uppermost 1 m layer of soil from the RUSWET-GRASS dataset [15,62] (http://www.ipf.tuwien.ac.at/insitu/). This dataset contains gravimetric measurements of natural grass available soil moisture from 1978 to 1985, taken at 130 meteorological stations in the former Soviet Union. Observations were made with a temporal resolution of about 10 days during the warm season, and once a month during winter. Four points in each flat observational plot (about 0.1 ha for each plot) are used for each data point, and the results averaged to give the data value. In this study, we used soil moisture observations from 8 sites which are close to our sampling plots and to the selected PDSI grids (Fig. 1A). In most cases, only warm season soil moisture data were available for these sites. Therefore, we evaluated and calculated the growing season (May-September) average soil moisture for each site and validated the relevant PDSI data. In the growing season, the average PDSI values correlated significantly and positively with the observed soil water content for the period 1978–1985 (Fig. *S1*, $r^2 = 0.34$, $p<0.001$), suggesting that the PDSI values can be used to indicate changes to soil water content in our study region.

The monthly soil water limitation (SWL) for this region for each biological year (running from October of the previous year to September of the current year) in the period 1928–2006 was estimated based on a simple water balance model:

$$SWL = PRE_i - PET_i$$

where PRE_i is the total precipitation for month i and PET_i is the potential evapotranspiration for month i, which is calculated using the Thornthwaite formula [63]. Specifically, there is surplus water when the monthly potential evapotranspiration is less than the total precipitation, otherwise there is a water shortage. The dynamic water balance was then calculated month by month and the total water limitation was estimated over months and seasons by summing the monthly SWL. Trends in monthly and seasonal climate series (i.e. temperature, precipitation, PDSI and SWL) were first identified by the Mann-Kendall non-parametric test [64,65]. Where a significant trend in a climate series was detected following the Mann-Kendall test, a linear regression was fitted and the slope estimated.

Relationships between Regional and Species Tree-growth and Climate Variables

A principal component analysis based on the correlation matrix was carried out for the 8 standard chronologies for the period 1928–2002, in order to evaluate regionally shared growth variability, which was assumed to correspond to the value of the first principal component (PC1) [66]. The broken stick test was performed to determine the significance of each of the principal components [67]. Temporal changes in shared growth variability were investigated using subintervals of 20 years with a 5-year lag. The subinterval of 20 years is required because the number of observations (years) must be greater than the number of variables (chronologies) in order to meet the requirements of the statistical analyses. The variance explained by PC1 was considered to be an indicator of the similarity between the 8 chronologies. Correlation analyses between the regional chronology (PC1) and species chronologies and climate series (monthly temperature, precipitation and PDSI) were conducted using the program DENDROCLIM2002 to identify the climate driver for regional and species tree-growth [68].

Climate Sensitivity of Tree-growth

In this study, we assessed tree growth sensitivity to climate using both annual sensitivity (S_x) and the proxy of soil water use efficiency (P_{SWUE}). The annual sensitivity (S_x) is the relative difference between one ring-width index and the next, and was calculated using the formula:

$$S_x = 2 \times |I_{t+1} - I_t| / (I_{t+1} + I_t).$$

where I_t is the ring-width index value for the year t [47]. This index is frequently used in dendroclimatology to show tree-growth sensitivity to climate [47]. Higher values for this index are indicative of greater interannual changes in ring-width, which imply a biased biological tree-growth rate. The proxy of soil water use efficiency was calculated from the following formula:

$$P_{SWUE} = I_t / (PDSI_t + 10).$$

where I_t is the ring-width index value for year t, and $PDSI_t$ is the biological-year annual average value for year t. We introduced a constant of 10 into the formula in order to offset negative PDSI values, as PDSI is a standard measure of surface moisture conditions, theoretically ranging from about -10 (dry) to 10 (wet) [59].

There are close positive relationships between both ring width index and NDVI [57,69], and NDVI and woody biomass [1,70] in boreal forests. Changes in ring width index therefore suggest variations in woody biomass in boreal forests, and changes in PDSI can indicate variations in the soil water content for our study

region, as illustrated above (Fig. *S1*). P_{SWUE} is a reasonable proxy for soil water use efficiency for tree growth. We further validated the constructed P_{SWUE} by comparing it against the ratio of BAI (a measure closely related to forest production) to soil water content for growing seasons over the period 1978–1985. The ratio of BAI to soil water content is a more physically grounded index that generally gives the true soil water use efficiency. For all the three species, there are close positive relationships between P_{SWUE} and the ratio of BAI to soil water content (Fig. *S2*, $p<0.05$ for all the three species). This confirms that the introduced measure of P_{SWUE} is a suitable and appropriate proxy for soil water use efficiency.

Conclusions

Our study found that hemi-boreal forests have suffered a marked decline in growth over the last two decades. Increasing soil water limitation during pre- and early growing seasons triggered by climate warming, contributed most significantly to this decline in growth. This rapid growth decline, and increased climate sensitivity, mean that these hemi-boreal forests may become more vulnerable if faced with greater drought stress in the future, as predicted by climate models [11]. In addition, different tree species differ in their growth patterns and responses to the changing climate. *P. sylvestris* suffers a more severe drought limitation than the larch species (*L. sibirica* and *L. gmelinii*), which can mostly be attributed to differences in soil water conditions. These findings provide valuable insights into the regional carbon cycle and vegetation dynamics, and could be useful for devising adaptive forest management strategies. The present study, combined with previous results [9,32,44], suggests that the hemi-boreal forests will retreat if faced with more severe drought stress and with potentially increasing levels of disturbance (e.g. fire and insect). Given the potential risks of climate-induced forest decline, increased attention should be paid to the management of adaptation options for enhancing forest resistance and resilience to projected climate stress. At stand level, we suggest reducing tree densities by thinning, thus moderating competition for water for the larch forests, and selecting more drought-resistant genotypes for pine forests. At a regional scale, we need to identify the areas where tree-growth decline is most likely to occur by monitoring climate trends, changes in permafrost and in the disturbance regime, and tree-growth patterns.

Supporting Information

Figure S1 Comparison between measured soil water contents of growing season for the 8 sites and the average PDSI values of growing season for the relevant grids during 1978–1985. Line in figure indicates the linear fit of this relationship ($y = 0.91x+11.77$, $r^2 = 0.34$, $p<0.001$).
(TIF)

Figure S2 Comparisons between the constructed P_{SWUE} and the ratio of basal area increments (BAI) to soil water contents for different species during 1978–1985. Lines in the figure indicate the linear fits of the relationships for *Pinus sylvestris* (grey line, $y = 0.2x+0.066$, $r^2 = 0.58$, $p<0.05$), *Larix sibirica* (black line, $y = 0.29x+0.018$, $r^2 = 0.60$, $p<0.05$), and *Larix gmelinii* (light grey line, $y = 0.18x+0.025$, $r^2 = 0.53$, $p<0.05$).
(TIF)

Figure S3 Scatter plots of principal component analysis (PCA) loadings of the 8 chronologies for the period 1928–2006. *P. sylvestris*, *L. sibirica* and *L. gmelinii* chronologies are marked as squares, triangles, and circles, respectively.
(TIF)

Acknowledgments

We thank Shilong Piao and Lixin Lv for their data management and Longbin He for the ring-width measurements. The authors are grateful to the two anonymous reviewers for their constructive comments.

Author Contributions

Conceived and designed the experiments: HYL OAA XCW. Performed the experiments: XCW HYL OAA NKB DVS. Analyzed the data: XCW OAA HYL. Contributed reagents/materials/analysis tools: XCW HYL OAA NKB DVS. Wrote the paper: XCW HYL OAA DLG.

References

1. Myneni RB, Dong J, Tucker CJ, Kaufmann RK, Kauppi PE, et al. (2001) A large carbon sink in the woody biomass of Northern forests. Proc Natl Acad Sci U S A 98: 14784–14789.
2. Goodale CL, Apps MJ, Birdsey RA, Field CB, Heath LS, et al. (2002) Forest carbon sinks in the Northern Hemisphere. Ecol Appl 12: 891–899.
3. Keeling CD, Chin JFS, Whorf TP (1996) Increased activity of northern vegetation inferred from atmospheric CO_2 measurements. Nature 382: 146–149.
4. Myneni RB, Keeling CD, Tucker CJ, Asrar G, Nemani RR (1997) Increased plant growth in the northern high latitudes from 1981 to 1991. Nature 386: 698–702.
5. Bogaert J, Zhou L, Tucker CJ, Myneni RB, Ceulemans R (2002) Evidence for a persistent and extensive greening trend in Eurasia inferred from satellite vegetation index data. J Geophys Res 107, doi:10.1029/2001JD001075.
6. Barber VA, Juday GP, Finney BP (2000) Reduced growth of Alaskan white spruce in the twentieth century from temperature-induced drought stress. Nature 405: 668–673.
7. Klos RJ, Wang GG, Bauerle WL, Rieck JR (2009) Drought impact on forest growth and mortality in the southeast USA: an analysis using Forest Health and Monitoring data. Ecol Appl 19: 699–708.
8. Allen CD, Macalady AK, Chenchouni H, Bachelet D, McDowell N, et al. (2010) A global overview of drought and heat-induced tree mortality reveals emerging climate change risks for forests. For Ecol Manage 259: 660–684.
9. Dulamsuren C, Hauck M, Leuschner C (2010) Recent drought stress leads to growth reductions in *Larix sibirica* in the western Khentey, Mongolia. Glob Chang Biol 16: 3024–3035.
10. Wilmking M, Juday GP, Barber VA, Zald HSJ (2004) Recent climate warming forces contrasting growth responses of white spruce at treeline in Alaska through temperature thresholds. Glob Chang Biol 10: 1724–1736.
11. Solomon S, Qin D, Manning M, Chen Z, Marquis M, et al. (2007) Contribution of Working Group I to the Fourth Assessment Report of the Intergovernmental Panel on Climate Change. Cambridge, United Kingdom, New York, USA.
12. Piovesan G, Biondi F, Di Filippo A, Alessandrini A, Maugeri M (2008) Drought-driven growth reduction in old beech (*Fagus sylvatica L.*) forests of the central Apennines, Italy. Glob Chang Biol 14: 1265–1281.
13. Silva LCR, Anand M, Leithead MD (2010) Recent widespread tree growth decline despite increasing atmospheric CO_2. PloS One 5: e11543. doi:10.1371/journal.pone.0011543.
14. Wang WZ, Liu XH, An WL, Xu GB, Zeng XM (2012) Increased intrinsic water-use efficiency during a period with persistent decreased tree radial growth in northwestern China: Causes and implications. For Ecol Manage 275: 14–22.
15. Vinnikov KY, Robock A, Speranskaya NA, Schlosser A (1996) Scales of temporal and spatial variability of midlatitude soil moisture. J Geophys Res 101: 7163–7174.
16. Kagawa A, Naito D, Sugimoto A, Maximov TC (2003) Effects of spatial and temporal variability in soil moisture on widths and $\delta^{13}C$ values of eastern Siberian tree rings. J Geophys Res 108, 4500, doi:10.1029/2002JD003019.
17. Dulamsuren C, Hauck M, Bader M, Osokhjargal D, Oyungerel S, et al. (2009) Water relations and photosynthetic performance in *Larix sibirica* growing in the forest-steppe ecotone of northern Mongolia. Tree Physiol 29: 99–110.
18. Sidorova OV, Siegwolf RTW, Saurer M, Shashkin AV, Knorre AA, et al. (2009) Do centennial tree-ring and stable isotope trends of *Larix gmelinii* (Rupr.) Rupr. indicate increasing water shortage in the Siberian north? Oecologia 161: 825–835.
19. Lloyd AH, Fastie CL (2002) Spatial and temporal variability in the growth and climate response of treeline trees in Alaska. Clim Change 52: 481–509.
20. Poutou E, Krinner G, Genthon C, de Noblet-Ducoudre N (2004) Role of soil freezing in future boreal climate change. Clim Dynam 23: 621–639.

21. Lawrence DM, Slater AG (2005) A projection of severe near-surface permafrost degradation during the 21st century. Geophys Res Lett 32, L24401, doi:10.1029/2005GL025080.
22. Anisimov O, Reneva S (2006) Permafrost and changing climate: The Russian perspective. AMBIO 35: 169–175.
23. Ye HC, Ellison M (2003) Changes in transitional snowfall season length in northern Eurasia. Geophys Res Lett 30, 1252, doi:10.1029/2003GL016873.
24. Sugimoto A, Yanagisawa N, Naito D, Fujita N, Maximov TC (2002) Importance of permafrost as a source of water for plants in east Siberian taiga. Ecol Res 17: 493–503.
25. Barnett TP, Adam JC, Lettenmaier DP (2005) Potential impacts of a warming climate on water availability in snow-dominated regions. Nature 438: 303–309.
26. Adam JC, Hamlet AF, Lettenmaier DP (2009) Implications of global climate change for snowmelt hydrology in the twenty-first century. Hydrol Process 23: 962–972.
27. Velisevich SN, Kozlov DS (2006) Effects of temperature and precipitation on radial growth of Siberian larch in ecotopes with optimal, insufficient, and excessive soil moistening. Russ J Ecol 37: 241–246.
28. Bunn AG, Goetz SJ, Fiske GJ (2005) Observed and predicted responses of plant growth to climate across Canada. Geophys Res Lett 32, L16710, doi:10.1029/2005GL023646.
29. Goetz SJ, Bunn AG, Fiske GJ, Houghton RA (2005) Satellite-observed photosynthetic trends across boreal north America associated with climate and fire disturbance. Proc Natl Acad Sci U S A 102: 13521–13525.
30. Bunn AG, Goetz SJ (2006) Trends in satellite-observed circumpolar photosynthetic activity from 1982 to 2003: The influence of seasonality, cover type, and vegetation density. Earth Interact 10: 1–19.
31. Bonan GB (2008) Forests and climate change: Forcings, feedbacks, and the climate benefits of forests. Science 320: 1444–1449.
32. Dulamsuren C, Hauck M, Khishigjargal M, Leuschner HH, Leuschner C (2010) Diverging climate trends in Mongolian taiga forests influence growth and regeneration of *Larix sibirica*. Oecologia 163: 1091–1102.
33. Dale VH, Joyce LA, McNulty S, Neilson RP, Ayres MP, et al. (2001) Climate change and forest disturbances. Bioscience 51: 723–734.
34. Soja AJ, Tchebakova NM, French NHF, Flannigan MD, Shugart HH, et al. (2007) Climate-induced boreal forest change: Predictions versus current observations. Glob Planet Change 56: 274–296.
35. Johnson EA, Miyanishi K, Weir JMH (1998) Wildfires in the western Canadian boreal forest: Landscape patterns and ecosystem management. J Veg Sci 9: 603–610.
36. Nealis VG, Regniere J (2004) Insect-host relationships influencing disturbance by the spruce budworm in a boreal mixedwood forest. Can J For Res 34: 1870–1882.
37. Rouault G, Candau JN, Lieutier F, Nageleisen LM, Martin JC, et al. (2006) Effects of drought and heat on forest insect populations in relation to the 2003 drought in western Europe. Ann For Sci 63: 613–624.
38. Westerling AL, Hidalgo HG, Cayan DR, Swetnam TW (2006) Warming and earlier spring increase western US forest wildfire activity. Science 313: 940–943.
39. Dulamsuren C, Hauck M, Bader M, Oyungerel S, Osokhjargal D, et al. (2009) The different strategies of *Pinus sylvestris* and *Larix sibirica* to deal with summer drought in a northern Mongolian forest-steppe ecotone suggest a future superiority of pine in a warming climate. Can J For Res 39: 2520–2528.
40. Kasyanova LN (2004) Ecology of plants in the Baikal region (water balance). Moscow: Nauka. (In Russian with English abstract).
41. Leshchikov FN (1993) Division into districts according to permafrost distribution. Baikal: Atlas. Moscow: Federal Service of Geodesy and Cartography of Russia. (In Russian with English abstract).
42. Badmaev NB, Kulikov AI, Korsunov VM (2006) Diversity of soils in the permafrost zone of Transbaikalia. Ulan-Ude: Buryat Scientific Center Press. (In Russian with English abstract).
43. Leithead MD, Anand M, Silva LCR (2010) Northward migrating trees establish in treefall gaps at the northern limit of the temperate-boreal ecotone, Ontario, Canada. Oecologia 164: 1095–1106.
44. Tchebakova NM, Parfenova E, Soja AJ (2009) The effects of climate, permafrost and fire on vegetation change in Siberia in a changing climate. Environ Res Lett 4, 045013, doi:10.1088/1748-9326/4/4/045013.
45. Laurent M, Antoine N, Joel G (2003) Effects of different thinning intensities on drought response in Norway spruce (*Picea abies* (L.) Karst.). For Ecol Manage 183: 47–60.
46. Li SG, Tsujimura M, Sugimoto A, Davaa G, Oyunbaatar D, et al. (2007) Temporal variation of $\delta^{13}C$ of larch leaves from a montane boreal forest in Mongolia. Trees-Struct Funct 21: 479–490.
47. Fritts HC (1976) Tree rings and climate. New York: Academic Press.
48. Holmes RL (1983) Computer assisted quality control in tree ring dating and measurement. Tree-Ring Bull 43: 69–78.
49. Cook ER (1985) A time-series analysis approach to tree-ring standardization [Ph.D. dissertation]. The University of Arizona Press, Tucson.
50. Wigley TML, Briffa KR, Jones PD (1984) On the average value of correlated time-series, with applications in dendroclimatology and hydrometeorology. J Clim Appl Meteorol 23: 201–213.
51. Cook ER, Kairiukstis LA (1990) Methods of dendrochronology. Netherland: Kluwer Academic Press.
52. Phipps RL, Whiton JC (1988) Decline in long-term growth trends of white oak. Can J For Res 18: 24–32.
53. Biondi F (1999) Comparing tree-ring chronologies and repeated timber inventories as forest monitoring tools. Ecol Appl 9: 216–227.
54. Hogg EH, Brandt JP, Kochtubajda B (2005) Factors affecting interannual variation in growth of western Canadian aspen forests during 1951–2000. Can J For Res 35: 610–622.
55. Paruelo JM, Epstein HE, Lauenroth WK, Burke IC (1997) ANPP estimates from NDVI for the central grassland region of the United States. Ecology 78: 953–958.
56. Fang JY, Piao SL, Zhou LM, He JS, Wei FY, et al. (2005) Precipitation patterns alter growth of temperate vegetation. Geophys Res Lett 32, L21411, doi:10.1029/2005GL024231.
57. Liang EY, Shao XM, He JC (2005) Relationships between tree growth and NDVI of grassland in the semi-arid grassland of north China. Int J Remote Sens 26: 2901–2908.
58. Mitchell TD, Jones PD (2005) An improved method of constructing a database of monthly climate observations and associated high-resolution grids. Int J Climatol 25: 693–712.
59. Dai A, Trenberth KE, Qian TT (2004) A global dataset of Palmer Drought Severity Index for 1870–2002: Relationship with soil moisture and effects of surface warming. J Hydrometeorol 5: 1117–1130.
60. Li JB, Gou XH, Cook ER, Chen FH (2006) Tree-ring based drought reconstruction for the central Tien Shan area in northwest China. Geophys Res Lett 33, L07715, doi:10.1029/2006GL025803.
61. Cook ER, Seager R, Cane MA, Stahle DW (2007) North American drought: Reconstructions, causes, and consequences. Earth-Sci Rev 81: 93–134.
62. Robock A, Vinnikov KY, Schlosser CA, Speranskaya NA, Xue YK (1995) Use of midlatitude soil-moisture and meteorological observations to validate soil-moisture simulations with biosphere and bucket models. J Clim 8: 15–35.
63. Thornthwaite CW (1948) An approach toward a rational classification of climate. Geogr Rev 38: 55–94.
64. Mann HB (1945) Nonparametric tests against trend. Econometrica 13: 245–259.
65. Kendall MG (1962) Rank correlation methods. New York: Hafner Publishing Company.
66. Andreu L, Gutierrez E, Macias M, Ribas M, Bosch O, et al. (2007) Climate increases regional tree-growth variability in Iberian pine forests. Glob Chang Biol 13: 804–815.
67. Holmes RL (1992) Dendrochronology program library. Version 1992–1. Tucson: Laboratory of Tree-Ring Research, University of Arizona.
68. Biondi F, Waikul K (2004) DENDROCLIM2002: A C++ program for statistical calibration of climate signals in tree-ring chronologies. Comput Geosci 30: 303–311.
69. Lopatin E, Kolstrom T, Spiecker H (2006) Determination of forest growth trends in Komi Republic (northwestern Russia): combination of tree-ring analysis and remote sensing data. Boreal Environ Res 11: 341–353.
70. Dong JR, Kaufmann RK, Myneni RB, Tucker CJ, Kauppi PE, et al. (2003) Remote sensing estimates of boreal and temperate forest woody biomass: carbon pools, sources, and sinks. Remote Sens Environ 84: 393–410.